

## Electronic Supplementary Information

### **An efficient multifunctional hybrid electrocatalyst: Ni<sub>2</sub>P nanoparticles on MOF-derived Co,N-doped porous carbon polyhedrons for oxygen reduction and water splitting**

Tingting Sun,<sup>a</sup> Shaolong Zhang,<sup>a</sup> Lianbin Xu,<sup>b</sup> Dingsheng Wang<sup>\*a</sup> and Yadong Li<sup>a</sup>

<sup>a</sup>Department of Chemistry, Tsinghua University, Beijing 100084, China

<sup>b</sup>State Key Laboratory of Organic-Inorganic Composites, Beijing University of Chemical Technology, Beijing 100029, China

\*Corresponding author: wangdingsheng@mail.tsinghua.edu.cn (D.W.)

## Table of Contents

1. Experiment section.....	S2-S4
2. References.....	S5
3. Supplementary Figures.....	S6-S14
4. Supplementary Tables .....	S15-S18

### 1. Experimental section

**Chemicals.** Cobalt nitrate hexahydrate ( $\text{Co}(\text{NO}_3)_2 \cdot 6\text{H}_2\text{O}$ , 99%, Alfa Aesar), zinc nitrate hexahydrate ( $\text{Zn}(\text{NO}_3)_2 \cdot 6\text{H}_2\text{O}$ , 98%, Alfa Aesar), 2-methylimidazole (MeIM, 99%, Acros Organics), nickel(II) chloride hexahydrate ( $\text{NiCl}_2 \cdot 6\text{H}_2\text{O}$ , 98%, Shanghai Aladdin), sodium hypophosphite ( $\text{NaH}_2\text{PO}_2$ , 99%, Shanghai Aladdin), Nafion D-521 dispersion (5% w/w in water and 1-propanol, Alfa Aesar), commercial Pt/C (20 wt% metal, Alfa Aesar), methanol (MeOH, Sinopharm Chemical), ethanol (EtOH, Sinopharm Chemical), cetyltrimethylammonium chloride solution (CTAC, 25 wt% in  $\text{H}_2\text{O}$ , Aldrich), tetraethyl orthosilicate (TEOS,  $\geq 99\%$ , Aldrich), KOH (analytical grade, Sinopharm Chemical), sulphuric acid ( $\text{H}_2\text{SO}_4$ , 98%, Beijing Chemical Reagents), and hydrofluoric acid (HF, 48-51%, Acros Organics) were used without any further purification. The distilled water used in all experiments was obtained through ion-exchange and filtration.

**Synthesis of ZnCo-BMOF.** In a typical procedure, 1.232 g MeIM was dissolved in 30 ml methanol to form a clear solution, which was subsequently injected into 30 ml of methanol containing  $\text{Co}(\text{NO}_3)_2 \cdot 6\text{H}_2\text{O}$  (0.546g) and  $\text{Zn}(\text{NO}_3)_2 \cdot 6\text{H}_2\text{O}$  (1.116 g) under ultrasound for 10 min at room temperature. The mixed solution was then transferred into 100 ml Teflon-lined stainless-steel autoclaves and heated at 120 °C for 4 h. The as-obtained precipitates were centrifuged and washed with methanol several times and dried in vacuum at 70 °C for overnight.

**Synthesis of ZnCo-BMOF@mesoSiO<sub>2</sub>.** 200 mg of the synthesized ZnCo-BMOF and 250 mg of MeIM were dispersed in 30 mL of  $\text{H}_2\text{O}$  and 15 mL of EtOH. After 10 min of ultrasonic treatment, 0.55 ml of CTAC was added and stirred for 20 min. Then, 0.4 ml TEOS was injected into the above solution and stirred for another 2 h. The product was collected by centrifugation, washed with EtOH and  $\text{H}_2\text{O}$ , and dried under a vacuum overnight. The product was named as ZnCo-BMOF@mesoSiO<sub>2</sub>.

**Synthesis of CoN-PCP.** The powder of ZnCo-BMOF@mesoSiO<sub>2</sub> was placed in a tube furnace and then heated to 920 °C for 3 h with a ramp rate of 5 °C min<sup>-1</sup> under flowing Ar gas, followed by cooling to room temperature naturally. The as-obtained powders were then immersed in aqueous HF (10 wt%) for 4 h to remove the SiO<sub>2</sub> protective coating. After washing thoroughly with EtOH and

H<sub>2</sub>O, the as-obtained Co,N-doped porous carbon polyhedrons (CoN-PCP) were dried oven overnight at 60 °C before further use.

**Synthesis of Ni<sub>2</sub>P/CoN-PCP.** 452 mg NiCl<sub>2</sub>•6H<sub>2</sub>O and 250 mg NaH<sub>2</sub>PO<sub>2</sub> were first dissolved in EtOH (20 mL) and H<sub>2</sub>O (40 mL) with stirring for 1 h at room temperature. After that, 15 mg of CoN-PCP sample was dispersed in a 3 mL of the above precursor solution and ultrasonicated for 1h, and then kept at 80 °C for 12 h. The dried powder was transferred into a ceramic boat and heated to 300 °C with a ramp rate of 5 °C min<sup>-1</sup> under an Ar flow and kept at 300 °C for 1 h. Afterwards, the product was naturally cooled to room temperature under Ar flow. Finally, the resulting material was washed by using EtOH and H<sub>2</sub>O for several times and dried under vacuum at 60 °C.

**Synthesis of Ni<sub>2</sub>P nanoparticles (NPs).** The Ni<sub>2</sub>P NPs were prepared by the same fabrication procedure as that for the synthesis of Ni<sub>2</sub>P/CoN-PCP but without adding CoN-PCP to the synthesis.

**Physicochemical characterization.** Powder X-ray diffraction patterns of samples were recorded using a Rigaku RU-200b X-ray powder diffractometer (XRD) with Cu K $\alpha$  radiation ( $\lambda = 1.5406 \text{ \AA}$ ). TEM images were performed on a Hitachi H-800 transmission electron microscope. The high-resolution TEM (HR-TEM), high-angle annular dark-field scanning transmission electron microscopy (HAADF-STEM) images and elemental mapping were recorded on a JEOL-2100F FETEM with electron acceleration energy of 200 kV. The scanning electron microscope (SEM) was carried out by a JSM-6700F SEM. Photoemission spectroscopy experiments (XPS) were performed at the Catalysis and Surface Science End station at the BL11U beamline of National Synchrotron Radiation Laboratory (NSRL) in Hefei, China. Elemental analysis of Co in the solid samples was detected by an Optima 7300 DV inductively coupled plasma optical emission spectrometry (ICP-OES).

**Electrochemical tests.** The electrochemical experiments were performed by a CHI 660E electrochemical workstation (Shanghai Chenhua Instrument Corp., China) in a three electrode cell with a catalyst covered glassy carbon rotating disk working electrode (5 mm in diameter), a Ag/AgCl (filled with 3.5 M KCl solution) reference electrode, and a graphite rod counter electrode. All the measured potentials in this work were converted to reverse hydrogen electrode (RHE) by the following equations:  $E_{\text{RHE}} = E_{\text{Ag/AgCl}} + 0.059 \text{ pH} + E^0_{\text{Ag/AgCl}}$  ( $E^0_{\text{Ag/AgCl}} = 0.197 \text{ V}$ ). Also, a resistance test was made and the 100% ohmic potential drop (iR) compensation was used during the tests. A 5 mg of the measured catalyst (i.e., Ni<sub>2</sub>P/CoN-PCP, Ni<sub>2</sub>P NPs, CoN-PCP, commercial Pt/C or RuO<sub>2</sub>) was dispersed in 960  $\mu\text{L}$  of a water-isopropanol solution (v/v 3:1) containing 40  $\mu\text{L}$  of 5 wt% Nafion solution by ultrasonication for at least 30 min. A portion of the ink suspension (10  $\mu\text{L}$ ) was then pipetted on the GC electrode, yielding a catalyst loading of  $\sim 0.26 \text{ mg cm}^{-2}$  after drying at room temperature.

For the ORR, the electrochemical experiments were conducted in O<sub>2</sub>-saturated 0.1 M KOH at room temperature. The RDE measurements were carried out under the rotation rates ranging from 400 to 2500 rpm at a scan rate of 5 mV·s<sup>-1</sup>. Cyclic voltammograms (CVs) were acquired within a potential range of 0.2-1.2 V vs. RHE at a scan rate of 50 mV s<sup>-1</sup>. Prior to the electrochemical measurement, the electrolyte was saturated with oxygen by bubbling O<sub>2</sub> for at least 30 min. The electron transfer numbers (*n*) and kinetic currents (*j<sub>k</sub>*) involved in the typical ORR process were calculated on the basis of the Koutecky-Levich equation:<sup>1</sup>

$$\frac{1}{j} = \frac{1}{j_k} + \frac{1}{j_d} = \frac{1}{j_k} + \frac{1}{B\omega^{1/2}}$$

$$B = 0.62nFC_0(D_0)^{2/3}\nu^{-1/6}$$

where *j* is the measured current density, *j<sub>k</sub>* and *j<sub>d</sub>* are the kinetic-limiting and diffusion-limiting current densities,  $\omega$  is the rotation speed in rpm, *n* is the electron transfer number, *F* is the Faraday constant (96485 C mol<sup>-1</sup>), *D<sub>0</sub>* is the diffusion coefficient of oxygen in the electrolyte (1.9 × 10<sup>-5</sup> cm<sup>2</sup> s<sup>-1</sup>),  $\nu$  is the kinetic viscosity of the electrolyte (0.01 cm<sup>2</sup> s<sup>-1</sup>), and *C<sub>0</sub>* is the bulk concentration of oxygen (1.2 × 10<sup>-6</sup> mol cm<sup>-3</sup>). The accelerated degradation testing was performed by running 2000 CV cycles on the electrode between 0.2 and 1.0 V vs. RHE with a scan rate of 100 mV s<sup>-1</sup>.

The OER and HER measurements were performed in an O<sub>2</sub>- or N<sub>2</sub>-saturated 1.0 M KOH solution, respectively. The electrocatalytic activity of the samples was examined by obtaining polarization curves using linear sweep voltammetry (LSV) with a scan rate of 5 mV·s<sup>-1</sup> while rotating the electrode at 1600 rpm. Cyclic voltammometry (CV) method was used to determine the electrochemical double-layer capacitances (*C<sub>dl</sub>*). Electrochemically active surface area could be evaluated from the slope of the plot of the charging current versus the scan rate, which was directly proportional to *C<sub>dl</sub>*. Electrochemical impedance spectroscopy (EIS) analysis was performed at different potentials in the frequency range from 10 kHz to 0.01 Hz using an amplitude of 5 mV. The accelerated durability tests for OER were conducted by potential cycling between 1.0 V and 1.6 V vs. RHE with a sweep rate of 100 mV s<sup>-1</sup> at a rotational speed of 1600 rpm for 2000 cycles. The accelerated durability tests for HER were conducted by potential cycling between -0.3 V and +0.2 V vs. RHE with a sweep rate of 100 mV s<sup>-1</sup> at a rotational speed of 1600 rpm for 2000 cycles. The chronoamperometry measurements were carried out for 20 hours at a constant potential of 1.55 V for OER and -0.1 V for HER.

The full electrolyzer configuration was assembled using two identical Ni<sub>2</sub>P/CoN-PCP electrodes and measured in a two-electrode cell in 1.0 M KOH solution with a carbon paper as the carrier (the catalyst loading is 2 mg·cm<sup>-2</sup>).

## 2. References

- 1 Y. J. Chen, S. F. Ji, Y. G. Wang, J. C. Dong, W. X. Chen, Z. Li, R. A. Shen, L. R. Zheng, Z. B. Zhuang, D. S. Wang and Y. D. Li, *Angew. Chem., Int. Ed.*, 2017, **56**, 6937.

### 3. Supplementary Figures

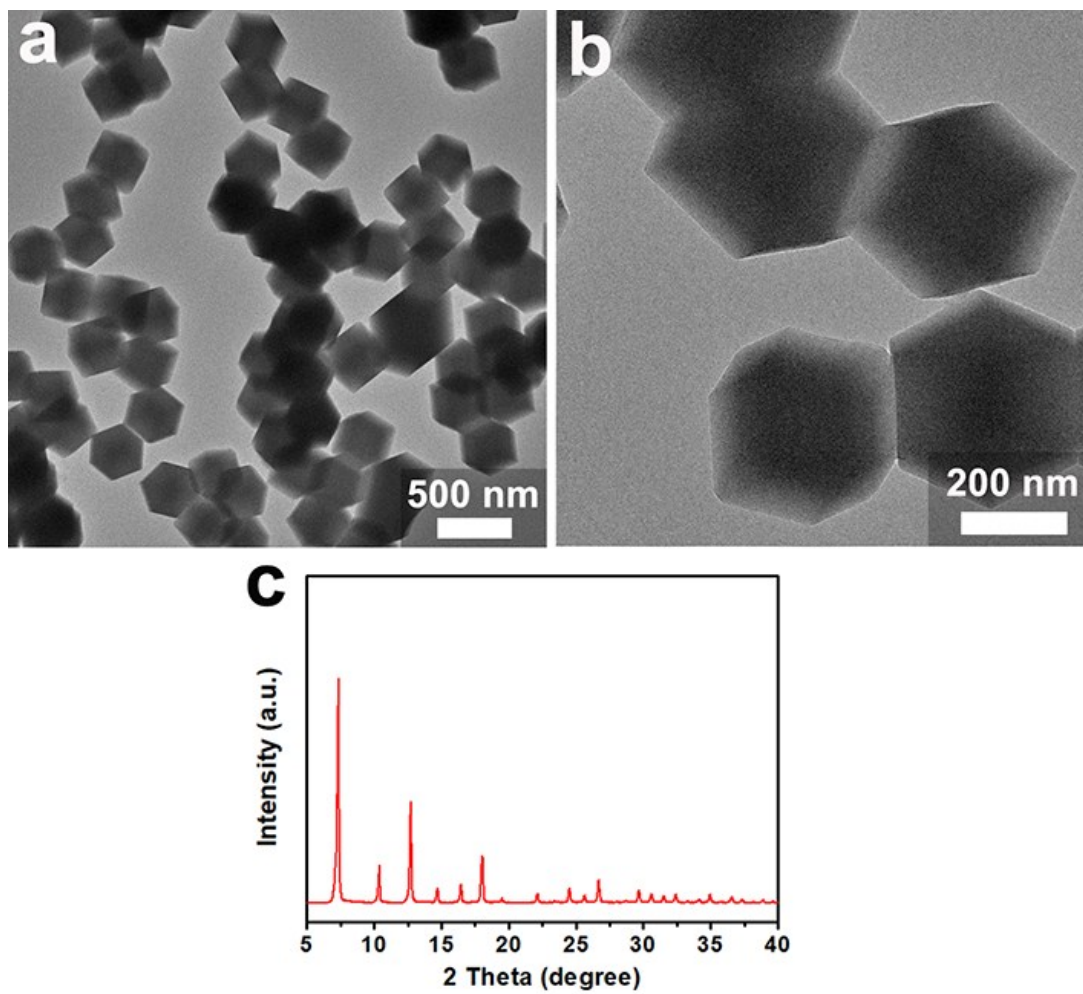


**Fig. S1** (a,b) TEM images and (c) XRD pattern of ZnCo-BMOF.

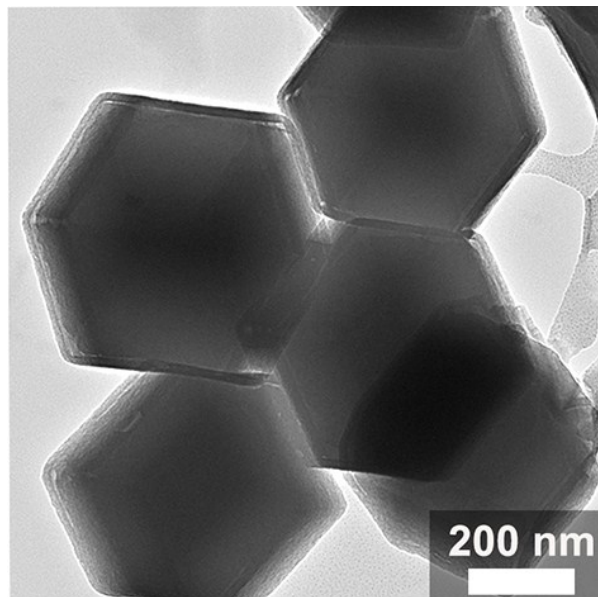


**Fig. S2** TEM image of ZnCo-BMOF@msoSiO<sub>2</sub>.

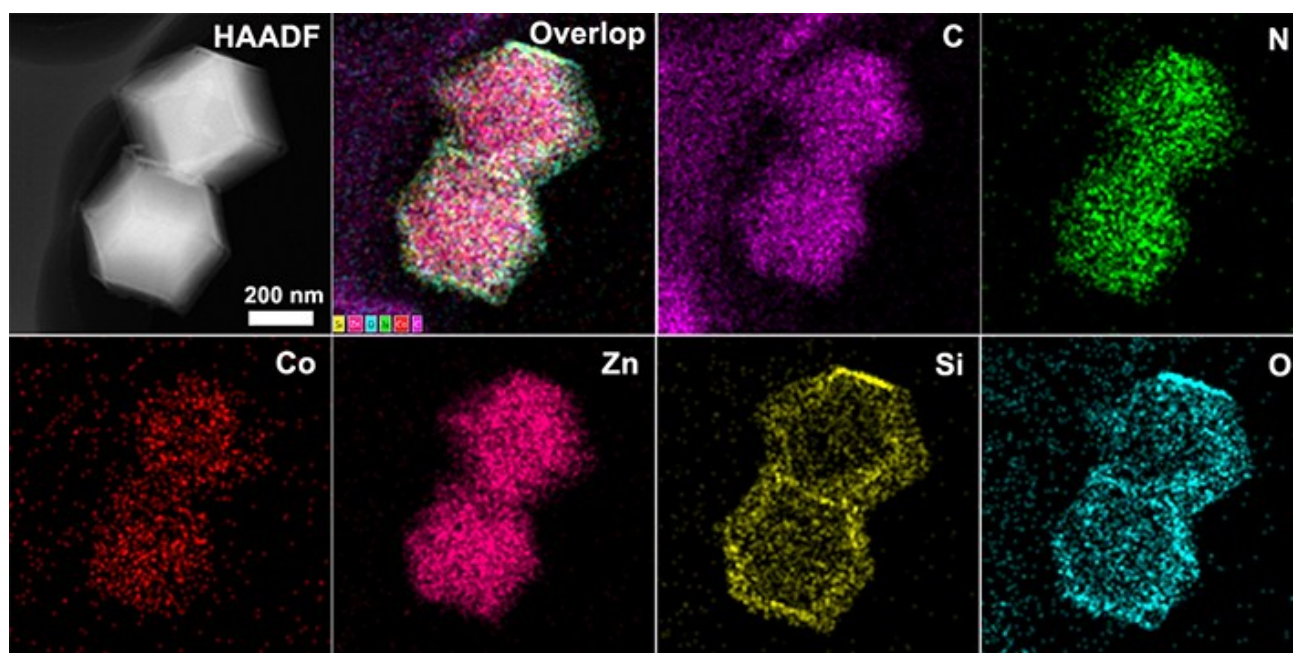


**Fig. S3** HAADF-STEM and corresponding EDS elemental mapping images of ZnCo-BMOF@msoSiO<sub>2</sub>

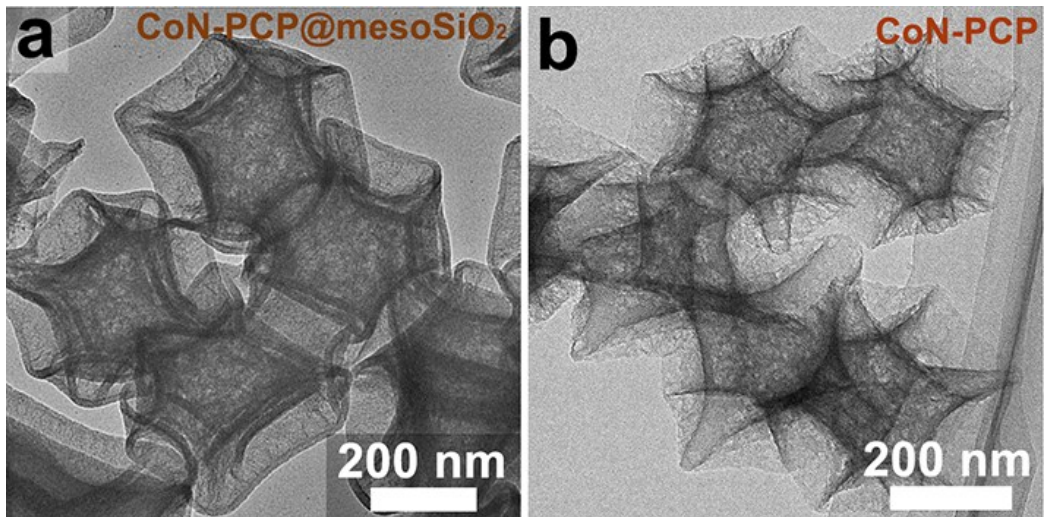


Fig. S4 TEM images of (a) CoN-PCP@mesoSiO<sub>2</sub> and (b) CoN-PCP.

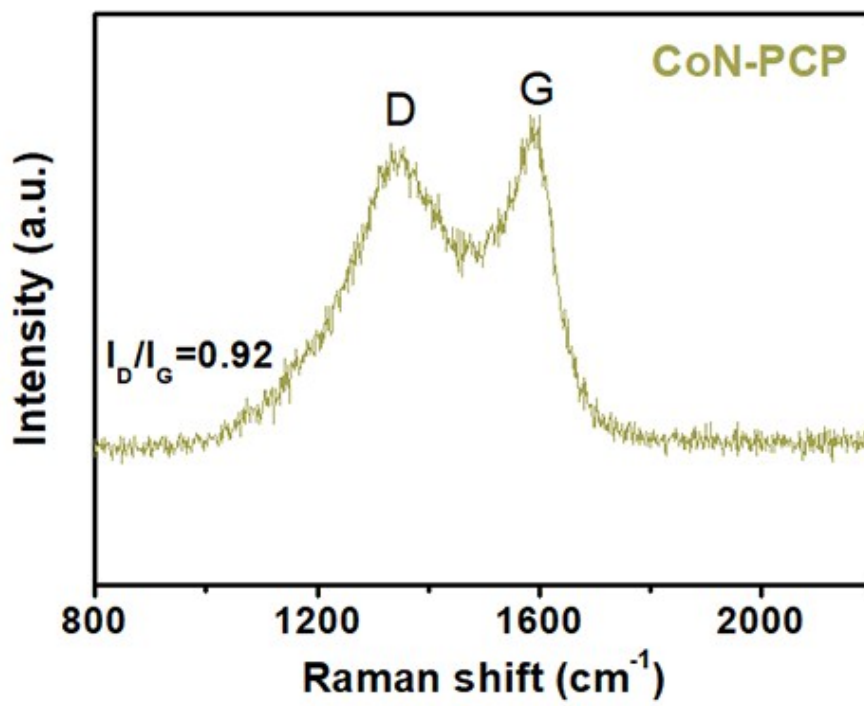
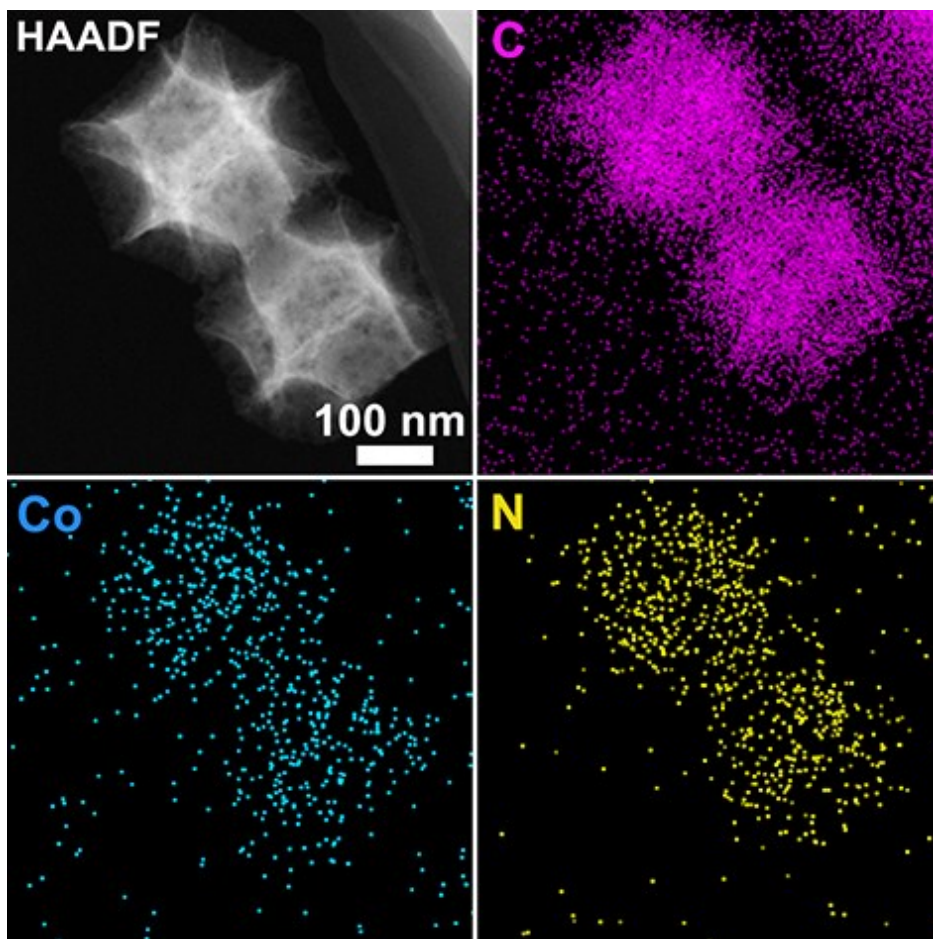
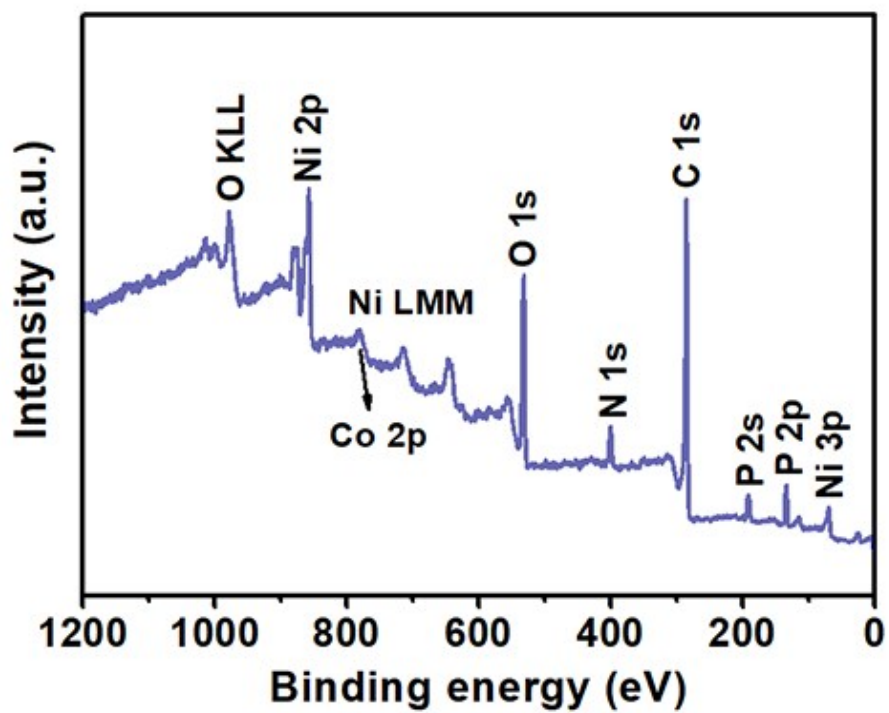


Fig. S5 Raman spectrum of CoN-PCP.



**Fig. S6** HAADF-STEM image of CoN-PCP and corresponding element maps showing the distribution of C (purple), Co (blue), and N (yellow).



**Fig. S7** XPS survey spectrum of Ni<sub>2</sub>P/CoN-PCP.

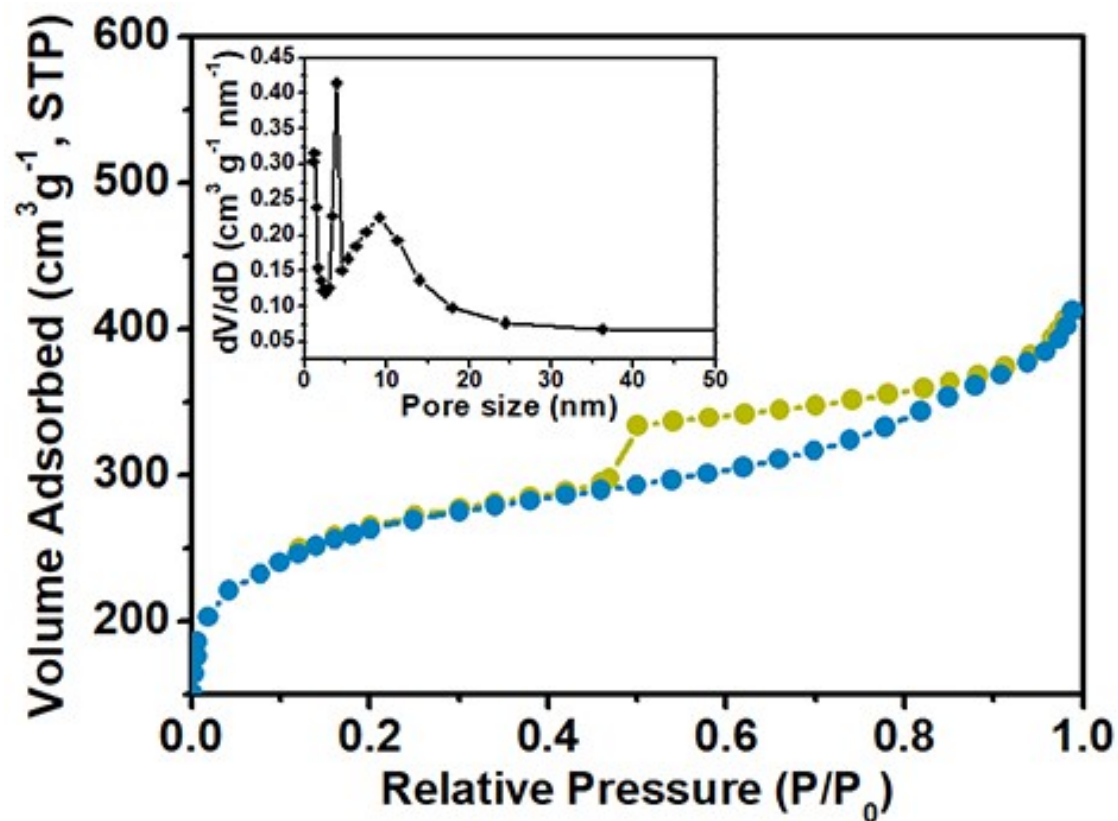


**Fig. S8** N<sub>2</sub> adsorption–desorption isotherms for Ni<sub>2</sub>P/CoN-PCP; the inset exhibits the corresponding pore size distribution based on the BJH method.

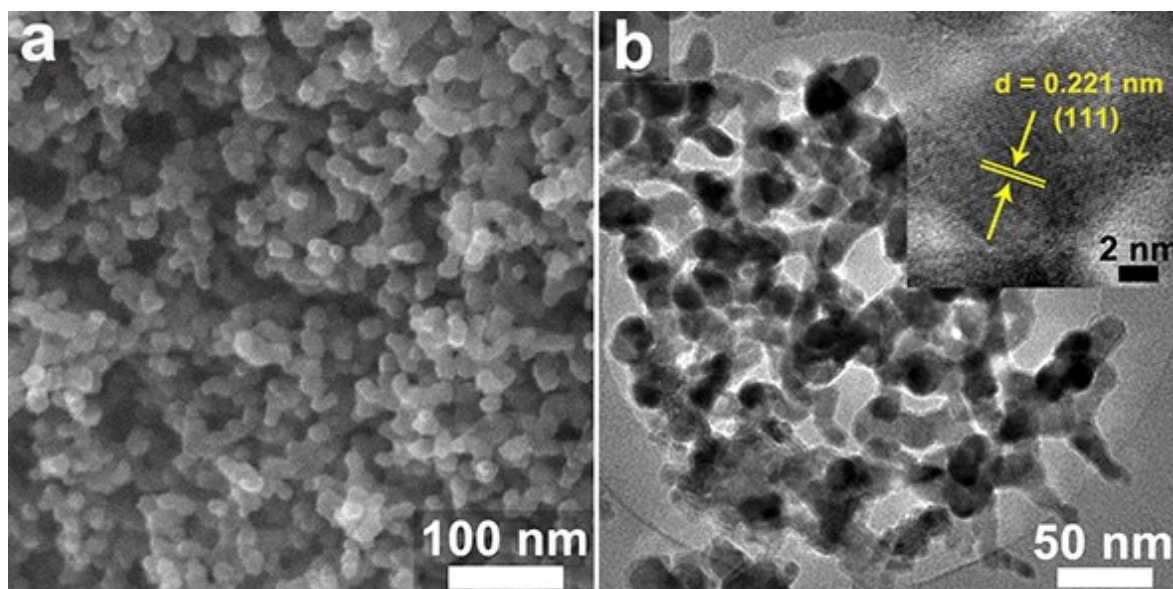


**Fig. S9** (a) SEM image, and (b) TEM image of Ni<sub>2</sub>P NPs.

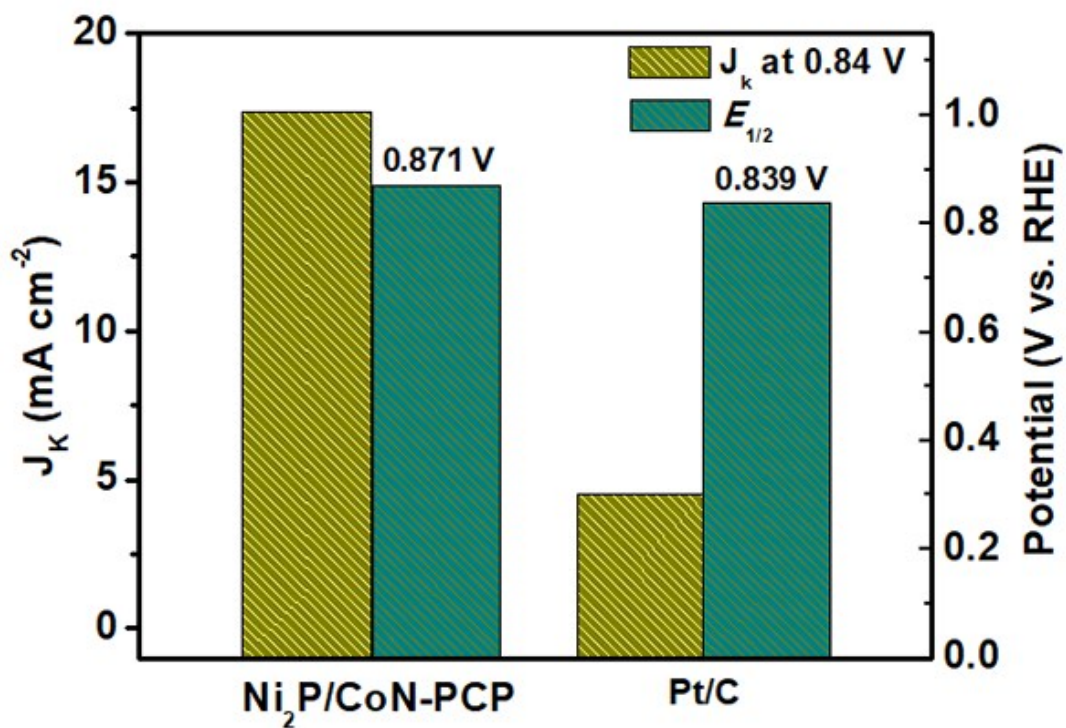


Fig. S10  $J_k$  at 0.84 V and  $E_{1/2}$  for different catalysts

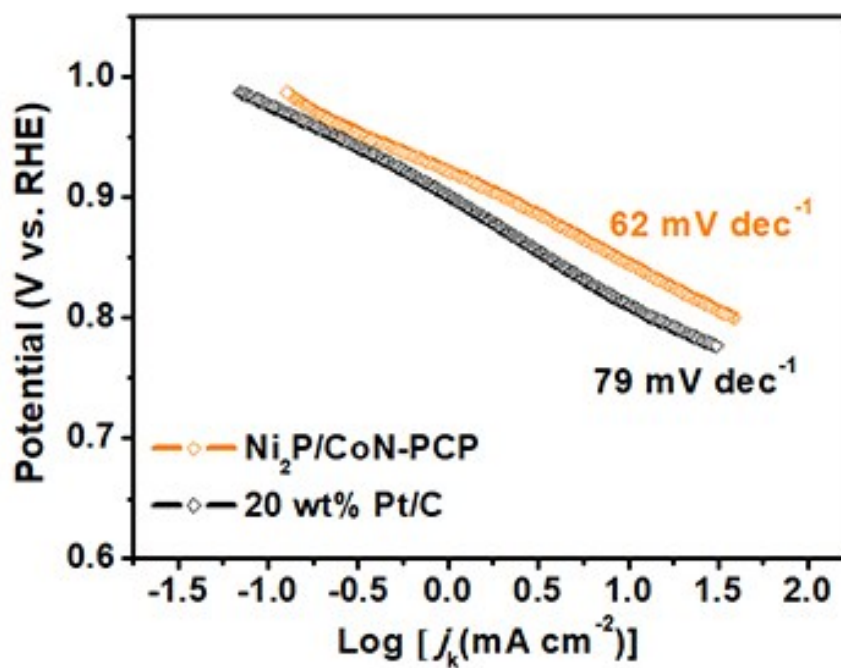


Fig. S11 Tafel slopes of different catalysts derived from the RDE LSV curves.

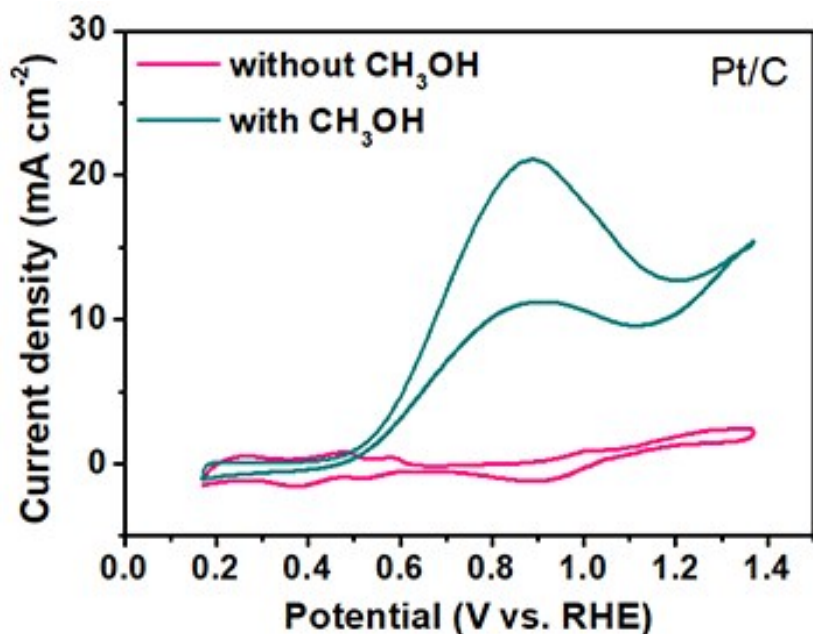


Fig. S12 CVs of Pt/C in  $O_2$ -saturated 0.1 M KOH without and with 1.0 M  $CH_3OH$ .

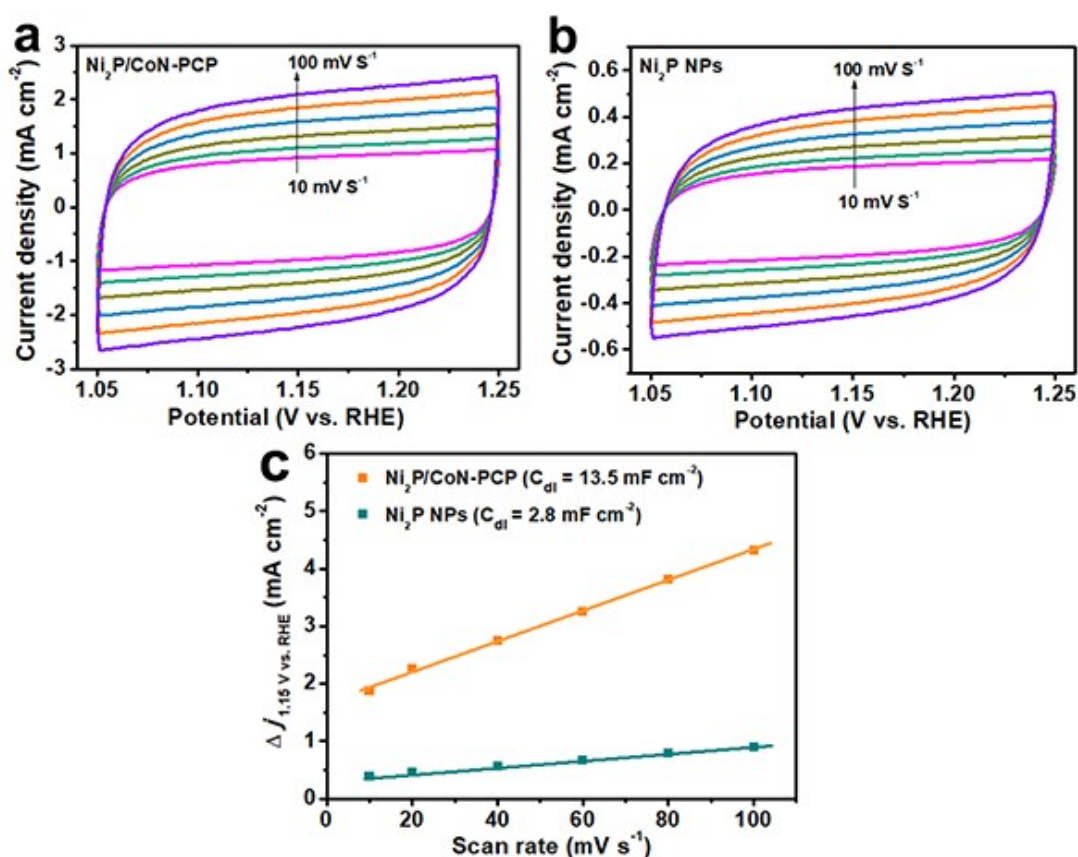
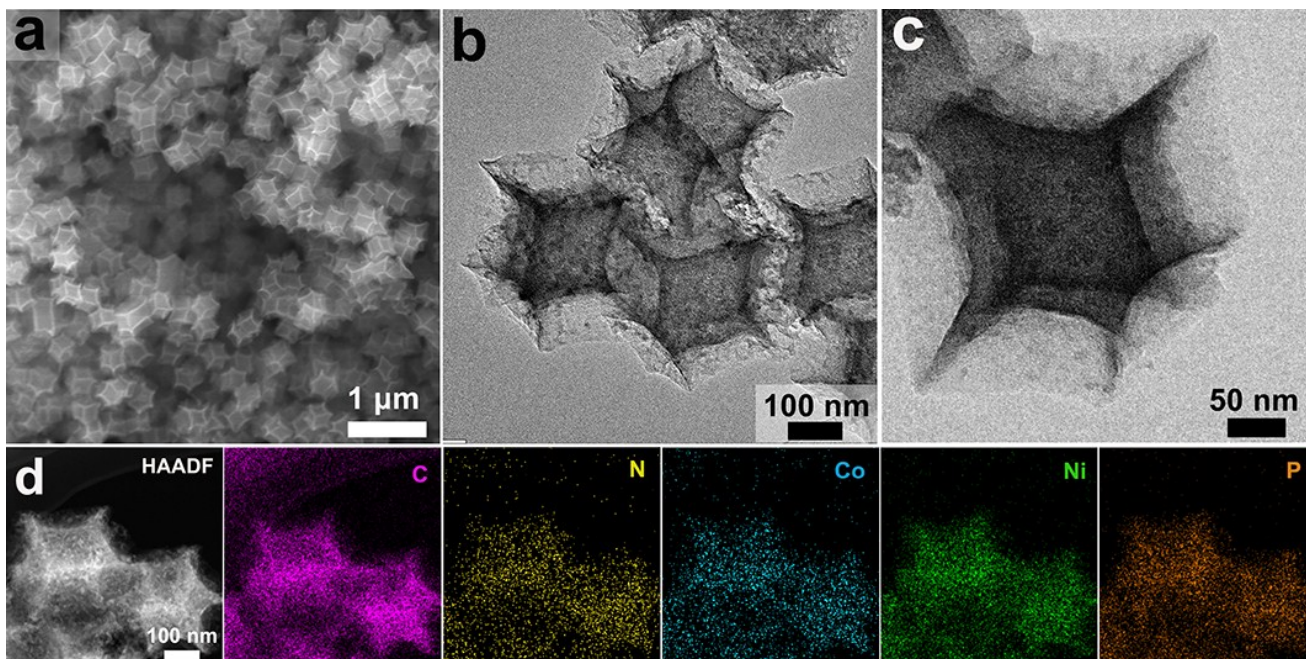
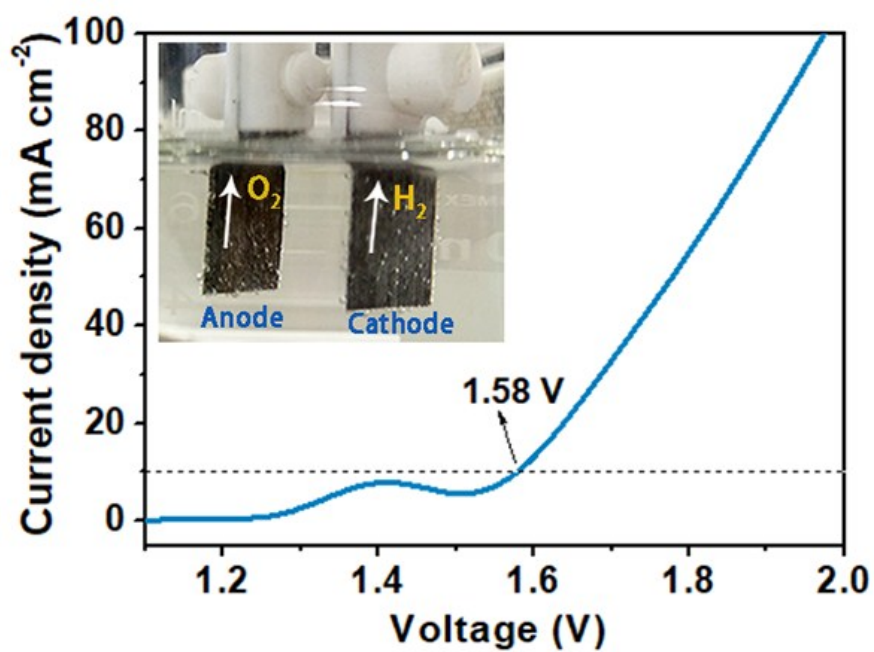


Fig. S13 Cyclic voltammetry (CV) of (a)  $Ni_2P/CoN-PCP$  and (b)  $Ni_2P$  NPs with different scan rates from 10 to 100  $mV \cdot s^{-1}$  in a non-faradic potential range of 1.05~1.25 V vs. RHE for OER in 1.0 M KOH solution. (c) The differences in current density variation ( $\Delta J = J_a - J_c$ ) at a potential of 1.15 V plotted against the scan rate fitted to a linear regression enables the estimation of  $C_{dl}$ .



**Fig. S14** (a) SEM image, (b,c) TEM images, and (d) HAADF-STEM and EDS elemental mapping images of the  $\text{Ni}_2\text{P}/\text{CoN-PCP}$  catalyst after CV durability test 1.0 M KOH for HER.



**Fig. S15** LSV curve of the  $\text{Ni}_2\text{P}/\text{CoN-PCP} \parallel \text{Ni}_2\text{P}/\text{CoN-PCP}$  electrode in 1.0 M KOH at a scan rate  $5 \text{ mV s}^{-1}$  for overall water splitting in a two-electrode system.

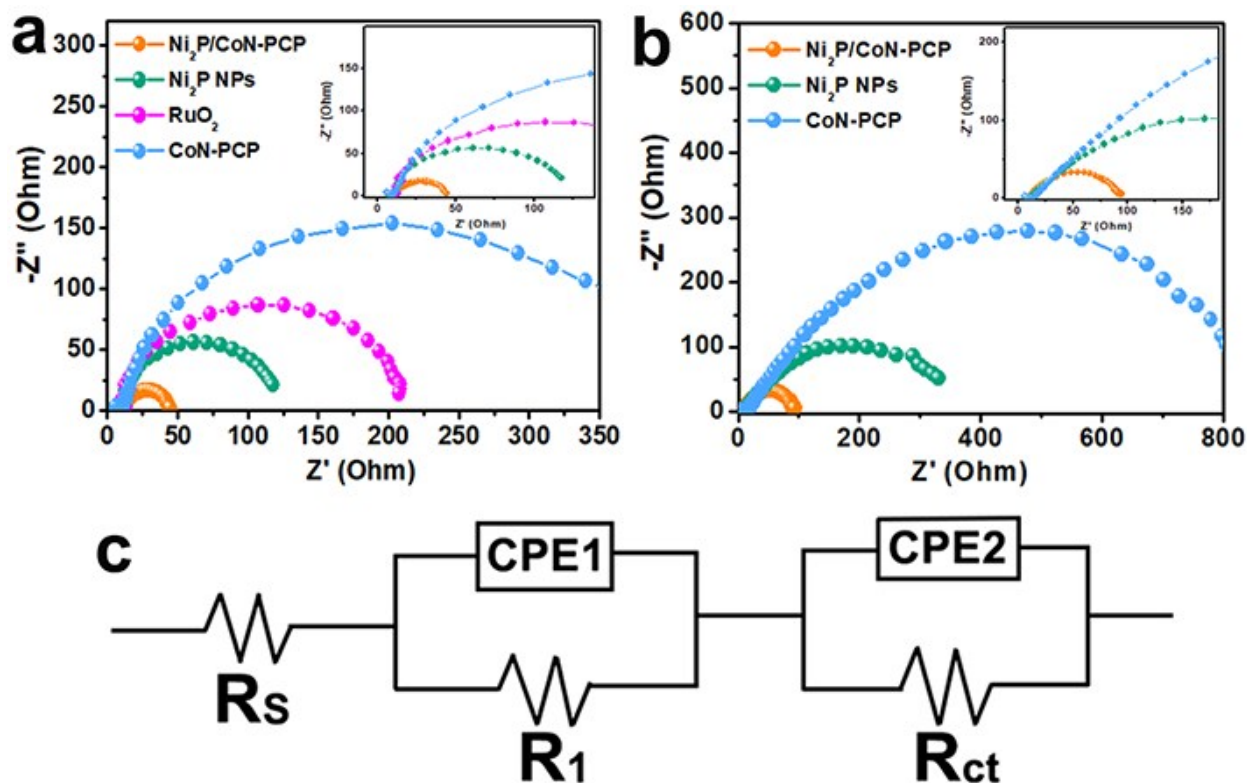


**Fig. S16** Nyquist plots of the  $\text{Ni}_2\text{P}/\text{CoN-PCP}$  and other compared catalysts for (a) OER with an overpotential of 370 mV and (b) HER with an overpotential of 100 mV. (c) Equivalent circuit model applied to fit the Nyquist plots, where  $R_s$  is the series resistance,  $R_{ct}$  is the charge transfer resistance,  $R_1$  relates to the interfacial resistance resulting from the electron transport between the catalyst and the GCE, and CPE1 and CPE2 represent the double layer capacitance.

## 4. Supplementary Tables

**Table S1.** ICP-OES analysis results of the Ni<sub>2</sub>P/CoN-PCP catalyst.

sample	Ni (wt%)	P (wt%)	Ni/P atomic ratio	Co (wt%)	N (wt%)
Ni <sub>2</sub> P/CoN-PCP	7.4	2.3	1.71	1.2	4.3

**Table S2.** Comparison of the electrocatalytic activity of Ni<sub>2</sub>P/CoN-PCP with other recently reported non-precious-metal electrocatalysts.

Catalyst	E (V) at 10 mA cm <sup>-2</sup> (1.0 M KOH)		<i>E</i> <sub>1/2</sub> (V) (0.1 M KOH)	Reference
	HER	OER	ORR	
Ni <sub>2</sub> P/CoN-PCP	<b>0.094</b>	<b>1.50</b>	<b>0.871</b>	<b>This work</b>
Fe-N <sub>4</sub> SAs/NPC	0.202	1.66	0.885	<i>Angew. Chem., Int. Ed.</i> , 2018, <b>57</b> , 1.
BA-TAP-Fe-800	0.33	1.55	0.85	<i>Chem. Commun.</i> , 2017, <b>53</b> , 2044.
CF-NG-Co	0.212	1.63	0.85	<i>J. Mater. Chem. A</i> , 2018, <b>6</b> , 489.
N, P, and F tri-doped graphene	0.52	1.80	0.72	<i>Angew. Chem., Int. Ed.</i> , 2016, <b>55</b> , 13296.
D-Co@CNG	0.205	1.59	0.81	<i>J. Mater. Chem. A</i> , 2017, <b>5</b> , 20882.
N, S co-doped graphitic sheets	0.310	1.56	0.87	<i>Adv. Mater.</i> , 2017, <b>29</b> , 1604942.
CoO <sub>x</sub> NPs/BNG	N.A.	1.525	0.805	<i>Angew. Chem. Int. Ed.</i> , 2017, <b>56</b> , 7121.
S-Co <sub>9-x</sub> Fe <sub>x</sub> S <sub>8</sub> @rGO-10	N.A.	1.52	0.84	<i>Small</i> , 2018, <b>14</b> , 1703748.
N-GCNT/FeCo-3	N.A.	1.73	0.92	<i>Adv. Energy Mater.</i> , 2017, <b>7</b> , 1602420.
NiFe-LDH/Co,N-CNF	N.A.	1.542 (0.1 M KOH)	0.79	<i>Adv. Energy Mater.</i> , 2017, <b>7</b> , 1700467.
Co <sub>3</sub> O <sub>4</sub> /N-rGO nanosheets	N.A.	1.72 (0.1 M KOH)	0.79	<i>Adv. Mater.</i> , 2018, <b>30</b> , 1703657.
FeN <sub>x</sub> -embedded PNC	N.A.	1.62 (0.1 M KOH)	0.86	<i>ACS Nano</i> , 2018, <b>12</b> , 1949.
S-GNS/NiCo <sub>2</sub> S <sub>4</sub>	N.A.	1.56 (0.1 M KOH)	0.88	<i>Adv. Funct. Mater.</i> , 2018, <b>28</b> , 1706675.
Co@NC-3/1	N.A.	1.57	0.87	<i>Adv. Energy Mater.</i> , 2018, <b>8</b> , 1702048.

meso/micro-FeCo-N <sub>x</sub> -CN-30	N.A.	1.6	0.886	<i>Angew. Chem., Int. Ed.</i> , 2018, <b>57</b> , 1856.
CoMn <sub>2</sub> O <sub>4</sub> -MnOOH NRs	N.A.	~1.61	0.8	<i>Chem. Commun.</i> , 2018, <b>54</b> , 4005.
multishelled Ni <sub>2</sub> P	0.098	1.50	N.A.	<i>Chem. Mater.</i> , 2017, <b>29</b> , 8539.
Mg-modified Ni <sub>2</sub> P	N.A.	1.51	N.A.	<i>ACS Catal.</i> 2017, <b>7</b> , 5450.
Ni <sub>2</sub> P@NPCNFs	0.104	N.A.	N.A.	<i>Angew. Chem. Int. Ed.</i> , 2018, <b>57</b> , 1963.
Ni <sub>2</sub> P-CoP	0.105	1.55	N.A.	<i>ACS Appl. Mater. Interfaces</i> , 2017, <b>9</b> , 23222.
CoP-2ph-CMP-800	0.36	1.60	N.A.	<i>Chem. Commun.</i> , 2016, <b>52</b> , 13483.
Ni-Co-P HNBS	0.107	1.50	N.A.	<i>Energy Environ. Sci.</i> , 2018, <b>11</b> , 872.
CoP/NCNHP	0.115	1.54	N.A.	<i>J. Am. Chem. Soc.</i> , 2018, <b>140</b> , 2610.
MoS <sub>2</sub> -Ni <sub>3</sub> S <sub>2</sub> HNRs/NF	0.098	1.479	N.A.	<i>ACS Catal.</i> , 2017, <b>7</b> , 2357.
CoP/rGO-400	0.105	1.57	N.A.	<i>Chem. Sci.</i> , 2016, <b>7</b> , 1690.
Co/NBC-900	0.117	1.532	N.A.	<i>Adv. Funct. Mater.</i> , 2018, <b>28</b> , 1801136.
NSWANs	0.132	1.496	N.A.	<i>Small</i> , 2017, <b>13</b> , 1701487.
NiCo <sub>2</sub> O <sub>4</sub>	0.110 (1.0 M NaOH)	1.52 (1.0 M NaOH)	N.A.	<i>Angew. Chem. Int. Ed.</i> , 2016, <b>55</b> , 6290.
Ni <sub>0.9</sub> Fe <sub>0.1</sub> /NC	>0.219	1.56	N.A.	<i>ACS Catal.</i> , 2016, <b>6</b> , 580.
VOOH nanospheres	0.164	1.50	N.A.	<i>Angew. Chem. Int. Ed.</i> , 2017, <b>56</b> , 573.
CoPS@NPS-C	0.191	1.55	N.A.	<i>J. Mater. Chem. A</i> , 2018, <b>6</b> , 10433.

**Table S3.** Values of elements in equivalent circuit resulted from fitting the EIS data.

Catalyst	Potential (V vs. RHE)	$R_s$ ( $\Omega$ )	$R_1$ ( $\Omega$ )	$R_{ct}$ ( $\Omega$ )
Ni <sub>2</sub> P/CoN-PCP	1.60	7.61	2.74	39.08
Ni <sub>2</sub> P NPs	1.60	8.15	5.15	107.6
RuO <sub>2</sub>	1.60	9.61	9.23	190.6
CoN-PCP	1.60	9.13	8.26	375.3
Ni <sub>2</sub> P/CoN-PCP	-0.1	7.58	3.87	86.97
Ni <sub>2</sub> P NPs	-0.1	7.39	5.92	303.7
CoN-PCP	-0.1	8.34	9.12	872.1